Earth's Future

RESEARCH ARTICLE
10.1029/2022EF003332

Key Points:
- CLIMAX is a climate-informed open source tool to assist energy transition with actionable strategies for wind and solar power deployment
- It allows leveraging climate-driven wind-solar complementarity to minimize the variability of their combined production
- In all European regions, optimal siting or sharing of wind and solar technologies would considerably increase the stability of the supply

Correspondence to:
S. Jerez,
sonia.jerez@um.es

Citation:
Jerez, S., Barriopedro, D., García-López, A., Lorente-Plazas, R., Somoza, A. M., Turco, M., et al. (2023). An action-oriented approach to make the most of the wind and solar power complementarity. *Earth's Future*, *11*, e2022EF003332. https://doi.org/10.1029/2022EF003332

Received 15 NOV 2022
Accepted 21 MAY 2023

Author Contributions:
Conceptualization: Sonia Jerez, Ricardo M. Trigo
Formal analysis: Sonia Jerez, David Barriopedro
Funding acquisition: Sonia Jerez, Marco Turco
Investigation: Sonia Jerez, Judit Carrillo, Ricardo M. Trigo
Methodology: Sonia Jerez, David Barriopedro, Raquel Lorente-Plazas, Andrés M. Somoza
Software: Sonia Jerez, Alejandro García-López, Raquel Lorente-Plazas, Andrés M. Somoza, Marco Turco

An Action-Oriented Approach to Make the Most of the Wind and Solar Power Complementarity

Sonia Jerez[1], David Barriopedro[2], Alejandro García-López[1,3], Raquel Lorente-Plazas[4], Andrés M. Somoza[1], Marco Turco[1], Judit Carrillo[5], and Ricardo M. Trigo[6,7]

[1]Department of Physics, University of Murcia, Murcia, Spain, [2]Instituto de Geociencias (IGEO), CSIC-UCM, Madrid, Spain, [3]Computational Earth Sciences – Earth Sciences Department, Barcelona Supercomputing Center, Barcelona, Spain, [4]Department of Meteorology, Meteored, Almendricos, Spain, [5]GOTA Group, University of La Laguna, San Cristobal de la Laguna, Spain, [6]Instituto Dom Luiz, Faculdade de Ciências, Universidade de Lisboa, Lisbon, Portugal, [7]Departamento de Meteorologia, Universidade Federal do Rio de Janeiro, Rio de Janeiro, Brazil

Abstract Solar and wind power are called to play a main role in the transition toward decarbonized electricity systems. However, their integration in the energy mix is highly compromised due to the intermittency of their production caused by weather and climate variability. To face the challenge, here we present research about actionable strategies for wind and solar photovoltaic facilities deployment that exploit their complementarity in order to minimize the volatility of their combined production while guaranteeing a certain supply. The developed methodology has been implemented in an open-access step-wise model called CLIMAX. It first identifies regions with homogeneous temporal variability of the resources, and then determines the optimal shares of each technology over such regions. In the simplistic application performed here, we customize the model to narrow the monthly deviations of the total wind-plus-solar electricity production from a given curve (here, the mean annual cycle of the total production) across five European domains. For the current shares of both technologies, the results show that an optimal siting of the power units would reduce the standard deviation of the monthly anomalies of the total wind-plus-solar power generation by up to 20% without loss in the mean capacity factor as compared to a baseline scenario with an evenly spatial distribution of the installations. This result further improves (up to 60% in specific regions) if the total shares of each technology are also optimized, thus encouraging the use of CLIMAX for practical guidance of next-generation renewable energy scenarios.

1. Introduction

The transition toward a decarbonized electricity system, powered by renewables, is urgently needed to achieve net greenhouse gas neutrality and so mitigate climate change, among other reasons (IPCC, 2018, 2021). However, most renewable energies, as far as they depend on weather and climate, present an inherent uncontrollable intermittency or temporal variability that hinders their integration in the energy mix. It makes necessary large investments in backup and storage systems, because the electricity production should be stable in time following the demand without much fluctuations. This issue led Antonini et al. (2022) to come up with the term "quantity-quality transition" to highlight that the optimal siting of the renewable generation facilities in a distributed network has to do not only with high capacity factors, but also with a high correlation between these and electricity demand (or residual demand), particularly under strict carbon emission constraints.

In order to face the challenge of the stability of a clean-energy supply system, here we focus on two variable renewable energies, wind and solar photovoltaic power, which should be key in the future energy deployment plans (European Commission, 2019). Moreover, they present a certain degree of spatio-temporal complementarity that could be exploited to reduce the variability of the combined wind-plus-solar production and mitigate the so-called power droughts (Brown et al., 2021; Jerez et al., 2013a; Solomon et al., 2020). For instance, the daily and annual cycles of the wind and solar resources are typically negatively correlated (Couto & Estanqueiro, 2021; Jerez et al., 2019; Schindler et al., 2020). Spatially, for a given energy, weather regimes and large-scale modes of climate variability have opposite fingerprints at different locations. The opposite effects of the North Atlantic Oscillation (NAO) on the renewable resources over southern and northern Europe represent a good example of this (e.g., Garrido-Pérez et al., 2020; Jerez et al., 2013b; Jerez & Trigo, 2013; van der Wiel et al., 2019).

10.1029/2022EF003332

Writing – review & editing: Sonia Jerez, David Barriopedro, Alejandro García-López, Raquel Lorente-Plazas, Andrés M. Somoza, Marco Turco, Judit Carrillo, Ricardo M. Trigo

Although wind and solar powers are mature technologies, and lots of production units are already supplying large portions of the demand in many countries (IRENA, 2020), an explosion of new installations is still to happen worldwide (e.g., European Commission, 2019). As the penetration of the variable renewables into the energy mix grows, it turns more vulnerable to climate variability. Hence, advances in the understanding and characterization of the climatic behavior of these resources, their complementarity and their optimal balance can be critical for the success of the upcoming facility deployment plans and, in the long-term, to accomplish with the Paris Agreement (IPCC, 2022).

Previous studies have already investigated the potential of the wind-solar complementarity to reduce the volatility of their combined production. Some of them assessed the advantages of hybrid (wind-solar) energy systems or explored local anticorrelations between these resources, focusing on their temporal-alone complementarity at a given location (e.g., Costoya et al., 2022; Couto & Estanqueiro, 2021; Jánosi et al., 2021; Liu et al., 2020). Others have dealt with the spatial-alone complementarity of a single resource (e.g., Mühlemann et al., 2022). Yet, a number of works did investigate the full potential of the spatio-temporal complementarity between wind and solar power for enlarging the stability of the supply, particularly over Europe (Frank et al., 2021; Grams et al., 2017; Santos-Alamillos et al., 2017; Wohland et al., 2021). Using national aggregate capacity factors, they explored the potential of a well-planed interconnected European power system to reduce the day-to-day, multi-day or multi-decadal supply variability of the combined wind and solar power generation. However, the literature has overlooked this issue at the monthly time-scale, even though the monthly anomalies of the wind and solar capacity factor series account for up to 20% of the whole variability in the series (Jerez et al., 2019). Besides, this time-scale is important to cope with climate extremes that can lead to prolonged peaks in demand, such as long-lasting cold-spells and heat waves, and low production in other renewable alternatives (e.g., hydropower), such as droughts. It is also relevant to address the growing demand from the energy sector for accurate seasonal predictions allowing risk anticipation and so the design of long-term action plans (Lledó et al., 2019).

Here we first deepen our understanding about the complementarity of the wind and solar capacity factors over Europe at the monthly time-scale with a climate-driven approach, uncovering links with the large-scale atmospheric circulation and its degree of influence. Then we present an action-oriented approach to quantify the benefits of a smart deployment of wind and solar facilities for pan-European regions, and the path to reach them. The originality of this climate-to-action solution relies on a powerful hybrid methodology which, in the first place, identifies regions with homogeneous temporal variability of the resources, and then determines the optimal shares of each technology over such regions. Full details on the method, including the open-source codes and an on-line interactive tool version, are available at http://climax.inf.um.es/ for its application beyond the limits of the illustrative academic exercise presented here, including different regions, time-scales and goals.

2. Data and Methods

2.1. Monthly Series of Wind and Solar Capacity Factors

We used here monthly series of wind and solar (photovoltaic) power potential (or capacity factors). These were constructed from hourly data of surface downward solar radiation, surface air temperature, 10-m height wind speed and 100-m height wind speed for the period 1979–2020 retrieved from the ERA5 reanalysis (Hersbach et al., 2020) with a spatial resolution of 0.25° (~30 km at the latitudes and longitudes considered here). Although ERA5 reanalysis may mask finer resolution terrain effects, particularly on the wind field over regions with complex topography (Jourdier, 2020), it has been proven reliable for both solar radiation (Urraca et al., 2018) and wind power modeling (Olauson, 2018). First we constructed hourly series of wind and solar capacity factors using simple relationships and power curves, as in Jerez and Trigo (2013) for the wind (considering turbines with 100-m hub height and 4, 12 and 24 m/s as cut-in, rated and cut-off speeds, respectively) and Jerez et al. (2015) for the solar power (including the effects of temperature and wind in the horizontal panel outputs). Then we computed accumulated monthly sums. The resulting monthly series were detrended and the monthly anomalies were obtained by subtracting the mean annual cycle. The analysis based on these series is restricted here to the European continent. In the case of the wind capacity factor series, the first grid cells off the coastline are also included in the analysis in order to consider offshore wind power installations.

2.2. Recurrent Atmospheric Patterns

Synoptic recurrent patterns were identified by performing a *k*-means clustering (e.g., Wilks, 2006) of the ERA5 monthly mean 500 hPa geopotential height (Z500) anomaly fields over the Euro-Atlantic sector (60W–40E, 25–75N) for the 1979–2020 period. The *k*-means method was applied to the 3 months of each season separately (i.e., a sample of 126 maps for each season). The approach assigns each month to one cluster based on the Euclidean distance (sum of squared differences) of the monthly Z500 anomalies with respect to the cluster's centroids. Clusters are determined iteratively by maximizing the distance between their centroids (inter-cluster distance) and minimizing the intra-cluster variance (the dispersion of maps within the same cluster). The method is applied with 1,000 iterations, thus allowing enough evolution of the centroids from the random initial seeds, but it requires predefining the number of clusters. The choice of four clusters was supported by the number of daily weather regimes employed in previous studies all-year round (e.g., Cassou et al., 2005; Cortesi et al., 2021; Michelangeli et al., 1995). This also provides a good compromise between a manageable number of clusters and their frequency of occurrence (five or more partitions yield low populated clusters).

2.3. Sub-Regions With Homogeneous Temporal Variability of the Capacity Factor Series

The user-oriented product presented here first clusters grid cells with similar temporal variability of the resources. For that we applied the methodology described in Lorente-Plazas et al. (2015) to the series of monthly anomalies of the wind and solar capacity factors, separately. First, a S-mode (spatial-mode) principal component analysis (PCA; von Storch & Zwiers, 2002) is performed. The correlation matrix is used to avoid the domination of locations with stronger variance. The number of retained components is chosen by means of a scree plot test (Cattell, 1966). A clustering is subsequently performed on the basis of the Euclidean distance between the retained eigenvectors from the PCA through a two-steps classification combining hierarchical and non-hierarchical algorithms. First, the hierarchical clustering, based on the Ward's minimum variance method (Ward, 1963), provides a first-guess classification. The resulting centroids then become the initial seeds for the non-hierarchical method applied here through the *k*-means algorithm (Hartigan & Wong, 1979).

2.4. Optimization Methods

The final objective of the CLIMAX tool is to identify optimal spatial distributions and shares of wind and solar photovoltaic power installations across a selected region. The optimization process pursues to minimize the deviations of the total wind-plus-solar production with respect to a given user-defined reference series or curve (e.g., a time series of electricity demand), while guaranteeing a certain minimum production. This is done under two frameworks that we call Optimal Distributions (OD) and Optimal Distributions and Shares (ODS). In the OD approach, the regional shares of wind and solar power are fixed values, so we worked only on their optimal spatial distribution across the sub-regions (i.e., which sub-regions and energy should be prioritized given the total regional shares). Differently, the ODS experiment is designed without constraints on the relative penetration (or share) of these energies.

Two algorithms, OD and ODS, were implemented in two python codes that work on minimizing the following function:

$$\sum_{k=1}^{\mathrm{NTT}}\left(\sum_{i=1}^{N_S} S_{Si}A_{Sik}+\sum_{j=1}^{N_W} S_{Wj}A_{Wjk}-B_k\right)^2$$

where A_{Sik}/A_{Wjk} are the input data of solar/wind power capacity factors corresponding to the sub-region *i*/*j* at time *k*, being N_S/N_W the number of sub-regions with homogeneous temporal variability and NTT the time-steps in the series, and B_k constitutes a reference time series of desired supply. The minimization of this function, hereafter optimization process, will provide the optimal values of S_{Si}/S_{Wj}, these being the shares of solar/wind power in the sub-region *i*/*j* that yield the best fit of the wind-plus-solar production—as given by the product of shares and the input capacity factors—to the provided reference series. In the application presented here, we aim to minimize the deviations with respect to the mean annual cycle of total production, and hence B_k is null at all *k* time-steps, since the capacity factors A_{Sik}/A_{Wjk} are expressed as monthly anomalies.

10.1029/2022EF003332

Table 1
Values of S_{SC}, S_{WC} and rs2w Used in the CLIMAX Applications Presented Here

Region	S_{SC}	S_{WC}	*rs2w*
R1	0.24	0.76	1.70
R2	0.57	0.43	1.90
R3	0.44	0.56	0.77
R4	0.32	0.68	0.34
R5	0.07	0.93	0.60

For the optimization process, we impose the following restrictions:

1. Positive share values, so:

$$S_{Si} \geq 0\, \forall i = 1, \cdots, N_S$$

$$S_{Wj} \geq 0\, \forall j = 1, \cdots, N_W$$

2. Total share = 1, that is:

$$\sum_{i=1}^{N_S} S_{Si} + \sum_{j=1}^{N_W} S_{Wj} = 1$$

3. Guarantee of a minimum production, given by:

$$\sum_{i=1}^{N_S} S_{Si} C_{Sik} + \sum_{j=1}^{N_W} S_{Wj} C_{Wjk} \geq M_k\, \forall k = 1, \cdots, \mathrm{NMP}$$

where C_{Sik}/C_{Wjk} refers to the absolute solar/wind power capacity factors (with the mean annual cycle included) for the sub-region *i/j* at time *k*, and M_k is user-defined. The implementation of this last condition allows guaranteeing a minimum production. In the examples of the main text, the C_S/C_W series contains the monthly annual cycle of the solar/wind power capacity factor data of each sub-region, and the *M* series the monthly annual cycle of the total (wind-plus-solar) power capacity factor in the whole target region according to a baseline scenario (further details in Section 3.2). Note that the number of time steps of the C_S, C_W and *M* series (NMP) should be the same (here is 12).

In the OD exercise, the total shares of each technology in the target region should be kept at pre-fixed values, S_{SC} for solar power and S_{WC} for wind power (Table 1 provides the values considered here). This adds the following conditions:

$$\sum_{i=1}^{N_S} S_{Si} = S_{SC}$$

$$\sum_{j=1}^{N_W} S_{Wj} = S_{WC}$$

For the ODS approach, we imposed here that the total share of solar power in the target region must be greater than the total share of wind power if the mean solar capacity factor is greater than the mean wind capacity factor in the region, and vice versa. This adds the following condition:

$$\sum_{i=1}^{N_S} S_{Si} \geq \sum_{j=1}^{N_W} S_{Wj} \text{ if } rs2w > 1$$

$$\sum_{i=1}^{N_S} S_{Si} \leq \sum_{j=1}^{N_W} S_{Wj} \text{ if } rs2w < 1$$

where *rs2w* is the ratio between the regional means of the solar power and the wind power capacity factors (see Table 1).

This later restriction to the solution space in the ODS approach can be overseen, if preferred. Also, additional restrictions—not imposed in the CLIMAX applications presented here—can be activated. Both OD and ODS codes admit minimum and maximum thresholds for the sub-regional shares of each energy, and also for the total regional shares in the case of ODS.

Both codes can be downloaded from http://climax.inf.um.es and further details are given there. We also provide there an additional couple of codes (OL, for Optimal Locations, and OLS, for Optimal Locations and Shares) which, unlike OD and ODS, work with amounts of installed capacity instead of shares of each energy.

3. Results

3.1. Understanding Complementarity: A Climatic Characterization With an Academic Approach

First we characterize the climatic behavior of the monthly anomalies of the wind and solar power capacity factors by assessing their responses to a portfolio of recurrent atmospheric patterns, a kind of monthly-extended weather regimes (see Section 2.2). Their centroids (i.e., the composites of Z500 anomalies for the months assigned to each cluster) are depicted in Figure 1 (labels C1–C4) for all seasons (December-to-February, DJF; March-to-May, MAM; June-to-August, JJA; and September-to-November, SON), where their frequency of occurrence (in % of total months) is also indicated. These patterns bear resemblance to the well-established daily weather regimes of the Euro-Atlantic sector (e.g., Michelangeli et al., 1995). In the overall, C1 captures the so-called Greenland Anticyclone (or negative phase of the NAO), C2 is a zonal flow or positive NAO-like pattern, C3 depicts European Blocking and C4 corresponds to the Atlantic Ridge configuration. Some patterns are identified in different seasons (e.g., Atlantic Ridge and European Blocking), but there are also seasonal variations, including the dominance of the canonical NAO pattern during the cold half of the year, and its transition to the summer NAO (top row; Folland et al., 2009). The zonal pattern (or NAO+, second row) is less stable across seasons, likely reflecting seasonal variations of the eddy-driven jet or a tendency for this cluster to agglutinate monthly fields that are loosely classified (e.g., close to climatology).

Figures 2 and 3 (second to fifth rows) show the seasonal anomalies in the solar and wind power monthly capacity factors, respectively, associated with each atmospheric pattern. Departures are expressed in percentage with

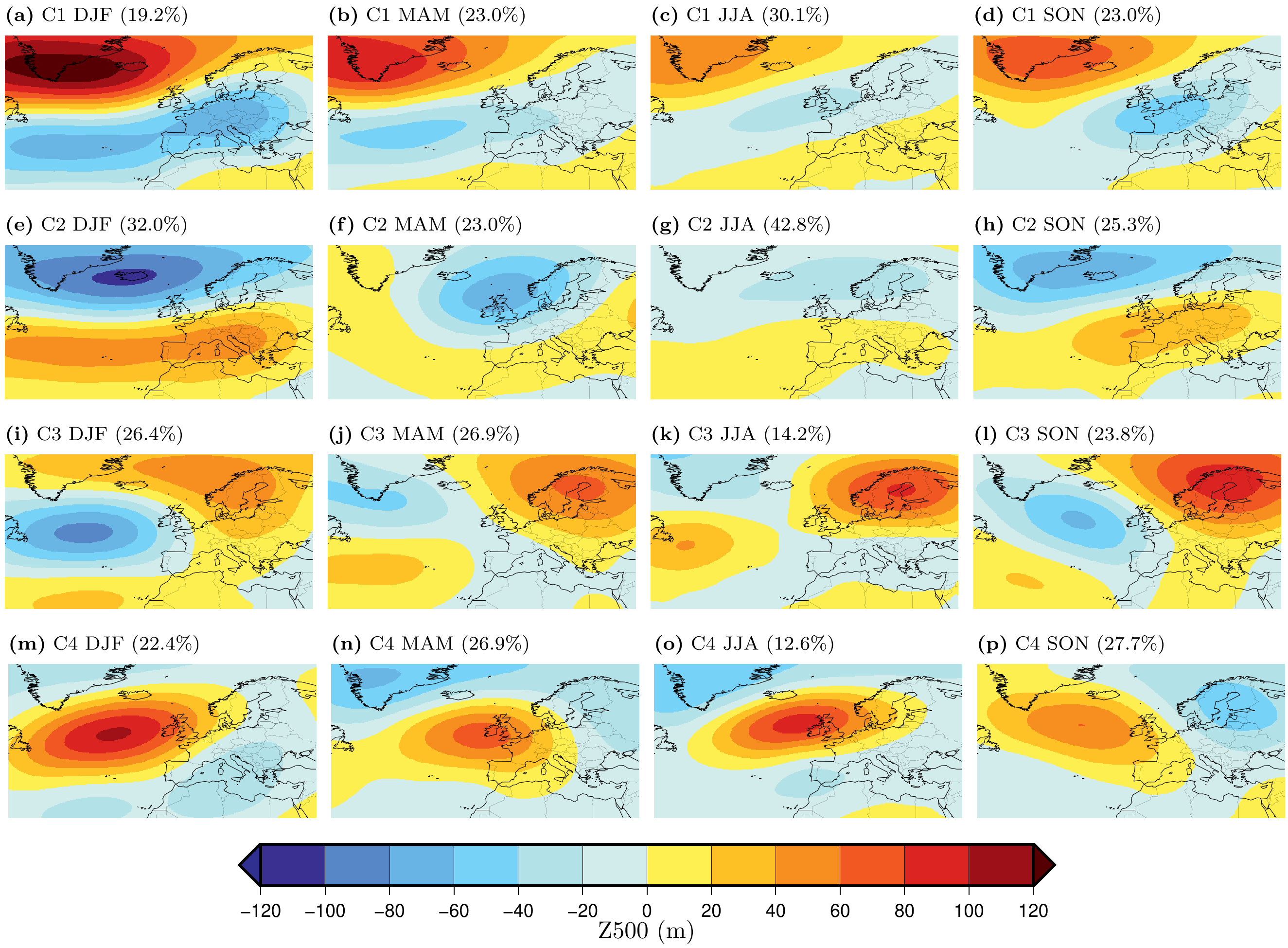

Figure 1. *Recurrent atmospheric patterns*. Seasonal climatologies (December-to-February [DJF], March-to-May [MAM], June-to-August [JJA] and September-to-November [SON] averages for 1979–2020) of the monthly anomalies of geopotential height at 500 hPa (Z500, units: m) for different recurrent atmospheric patterns (C1–C4 from top to bottom). In percentage, the frequency of occurrence of each configuration.

10.1029/2022EF003332

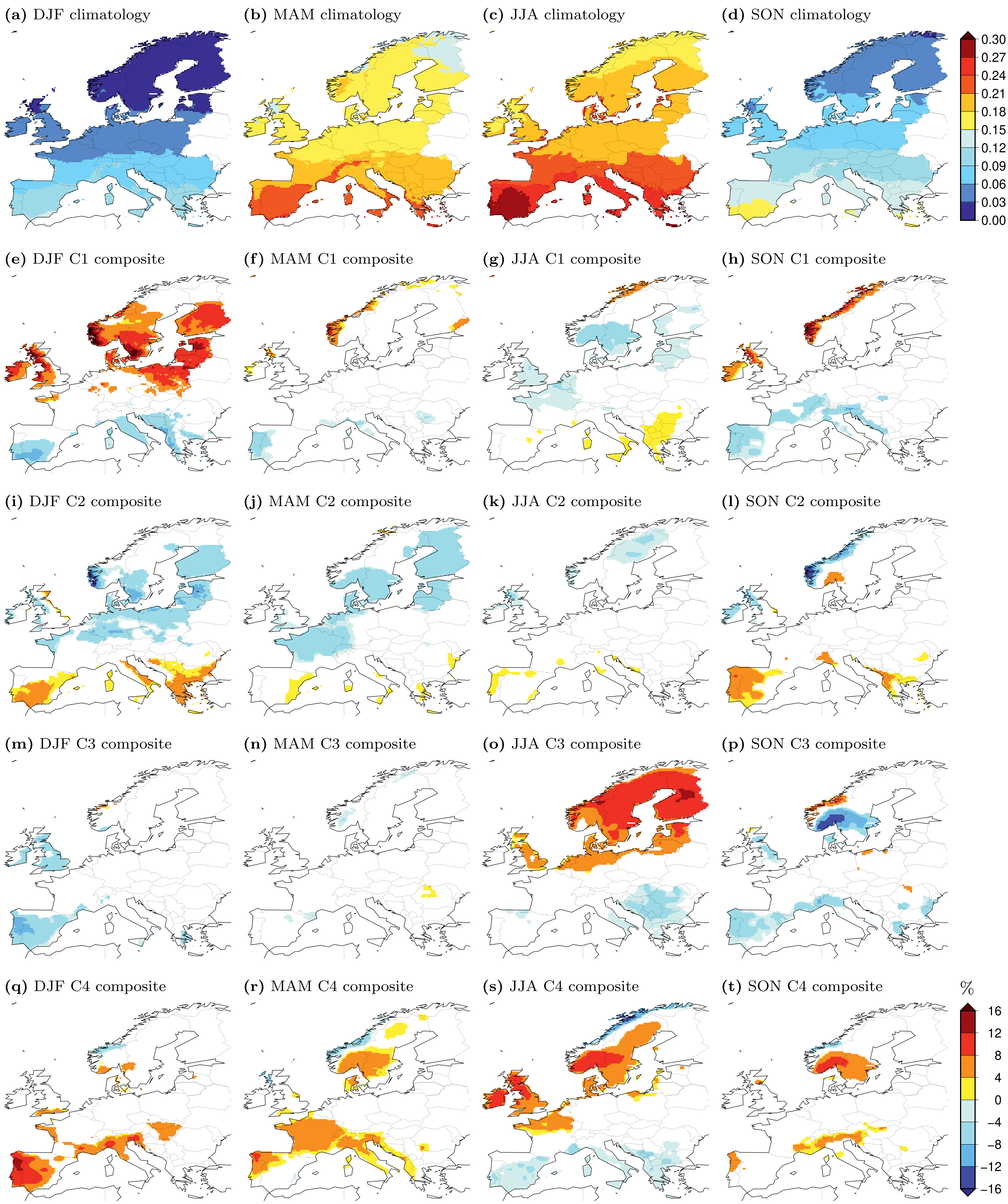

Figure 2. *Solar power under recurrent atmospheric patterns*. First row shows the seasonal climatologies (December-to-February [DJF], March-to-May [MAM], June-to-August [JJA] and September-to-November [SON] averages for 1979–2020) of the solar (photovoltaic) power capacity factor (dimensionless). Second to fifth rows show the composites of the anomalies in this variable (units: % deviation from the mean state) for recurrent atmospheric patterns (C1–C4 from top to bottom). Only statistically significant differences at $p < 0.05$ are shown. The statistical significance of the anomalies was assessed using the R *t.test* function (https://www.rdocumentation.org/packages/stats/versions/3.6.2/topics/t.test; two-sided). The studied area is restricted to the shadowed areas in panels (a–d).

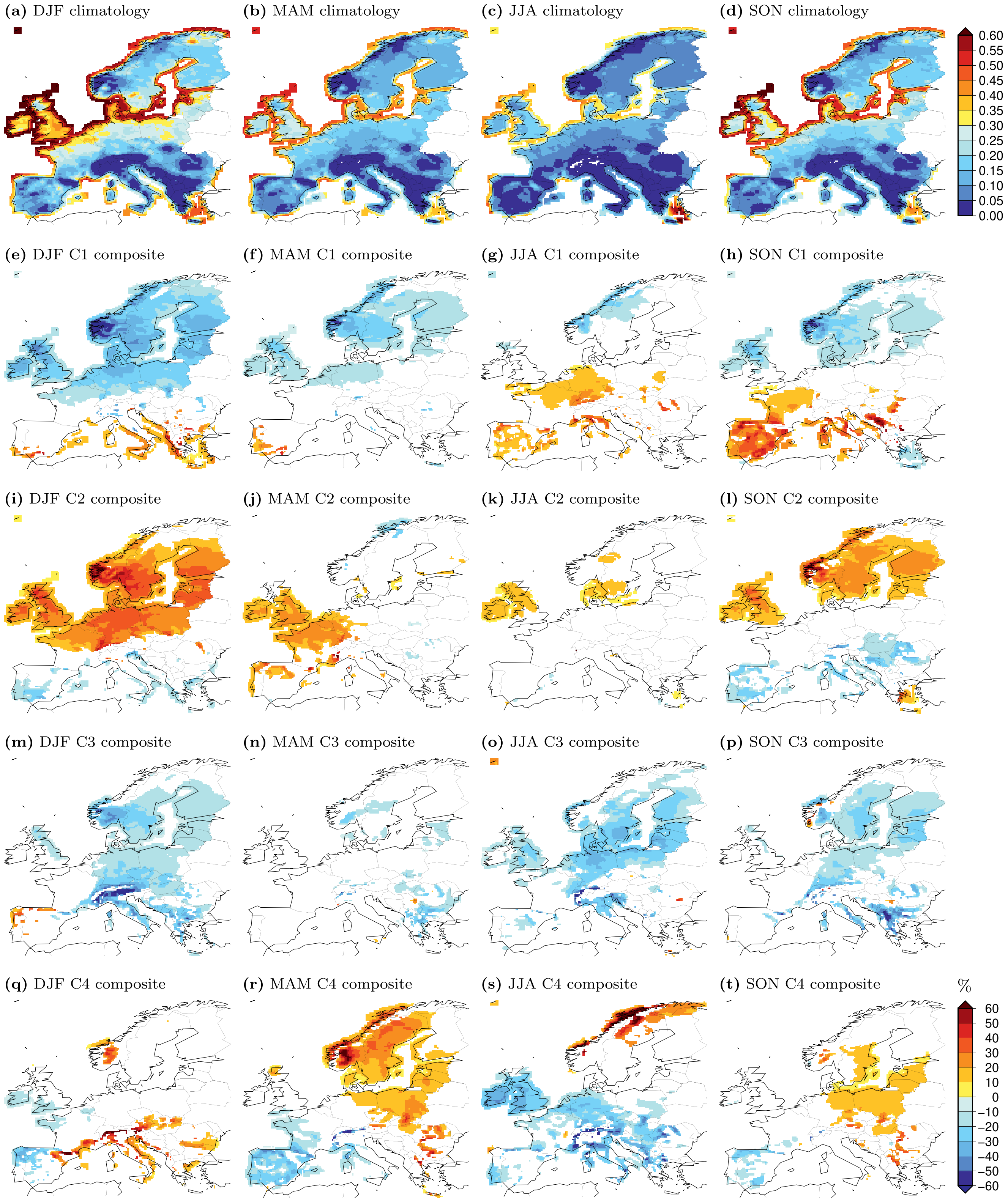

Figure 3. *Wind power under recurrent atmospheric patterns*. As Figure 2 for the wind power capacity factor. The studied area includes the first line of grid points off-shore.

10.1029/2022EF003332

respect to the climatological mean solar and wind power capacity factors of each season (top rows in Figures 2 and 3). The results are consistent with the documented behavior of wind- and solar-related fields under specific atmospheric circulation constraints (Garrido-Pérez et al., 2020; Jerez et al., 2013a; Jerez & Trigo, 2013; van der Wiel et al., 2019; Wohland et al., 2021). Although significant signals can be restricted to small regions of Europe, for both energies and all seasons, we do find recurrent situations (typically more than one atmospheric pattern) with negative and positive signals over different areas. Although these opposite responses typically occur in far away regions, from a spatially aggregated perspective, positive departures in power capacity factors can compensate for the negative ones, and this is what we call spatial complementarity. Therefore, one can think on an effective spatial balance of energy resources at continental or regional scale. On the other hand, comparison of the individual maps of Figures 2 and 3 confirm that, in general terms, a deficit in one energy turns in surplus in the other. Therefore, locally, wind and solar power tend to show opposite responses to a given atmospheric configuration (in agreement with the documented behavior on shorter temporal scales; see e.g., the references above). Accordingly, there is also a solid basis for the so-called temporal complementarity on monthly scales.

If we directly look at the temporal correlations between the series of monthly anomalies in the wind and solar power capacity factors (Figure 4, first row), forgetting about the particular influence of atmospheric conditions, negative signals (largely in the range −0.4 to −0.6, eventually up to −0.8) dominate, albeit accompanied by positive values of similar magnitude over some regions, mostly Mediterranean. Ultimately, the variability of these times series is largely the result of the temporal sequence of atmospheric patterns with distinctive spatial signatures in wind and solar energies. Hence, their complementarity should be, to a large extent, an intrinsic feature of wind and solar energies, regardless of the dominant atmospheric pattern. To show this, Figure 4 (second to fifth rows) shows the percentage of time (months in the season) over the analyzed period when a negative anomaly in wind power coincides with a positive anomaly in the solar one, and vice versa, under the influence of each atmospheric configuration. The predominance of yellows and reds in these maps means a generalized tendency for local compensation of wind and solar energy across Europe more than 50% of the time. However, there are regions (e.g., Mediterranean areas) where the signals indicate low synchronicity of power anomalies, as denoted by the bluish tones. Similarly, the degree of local complementarity is modulated by the atmospheric pattern: in some regions wind and solar powers can either add or oppose each other depending on the atmospheric configuration (e.g., winter power in Scandinavia under C1 and C4 patterns). Therefore, we can only be moderately confident on the local temporal complementarity of both energies, at least on the monthly time-scale assessed here.

In summary, these analyses come to confirm an overall complementarity, both spatially and temporally, between both powers. However, the balance varies seasonally, from region to region and with the dominant atmospheric pattern, encouraging further research efforts to take a transferable advantage of it. While this prevents universal solutions, actionable strategies are still possible on regional scales by combining knowledge on spatial and temporal complementarity. Below we explore new avenues through a hybrid (statistical-climate) approach that exploits this climate-driven complementarity to yield optimal balances of wind and solar energies on regional scales.

3.2. Leveraging Complementarity With CLIMAX: An Action-Oriented Approach

In view of the above results, we adopted a statistical approach to provide practical guidance to reduce the temporal variability of the joint wind-plus-solar power production at the regional level. Based on climatological arguments (see previous section), we considered five contiguous (geographically connected) regions, namely south-west (R1, Iberia), south-east (R2, Italy and the Balkans), central (R3), north-west (R4, the UK) and north-east (R5, Scandinavia) Europe (see Figure 5). For each region, the spatial distributions of the installations are optimized, making the most from the two concepts above (spatial and temporal complementarity) in an underlying way. Actually, the goal is to reduce the variance of the differences between production and demand, or between actual (fluctuating) and desired (stable) production. For the illustrative academic application performed here, the reference time series of desired production is simply set to the mean annual cycle of total (wind-plus-solar) production, rather than to the electricity usage in each region. Thus, this approach ultimately involves minimizing the variance of the monthly anomalies of the total (wind-plus-solar) power output in order to guarantee a stabilized production based on optimal balance of energies. The optimization is done so that a certain minimum production

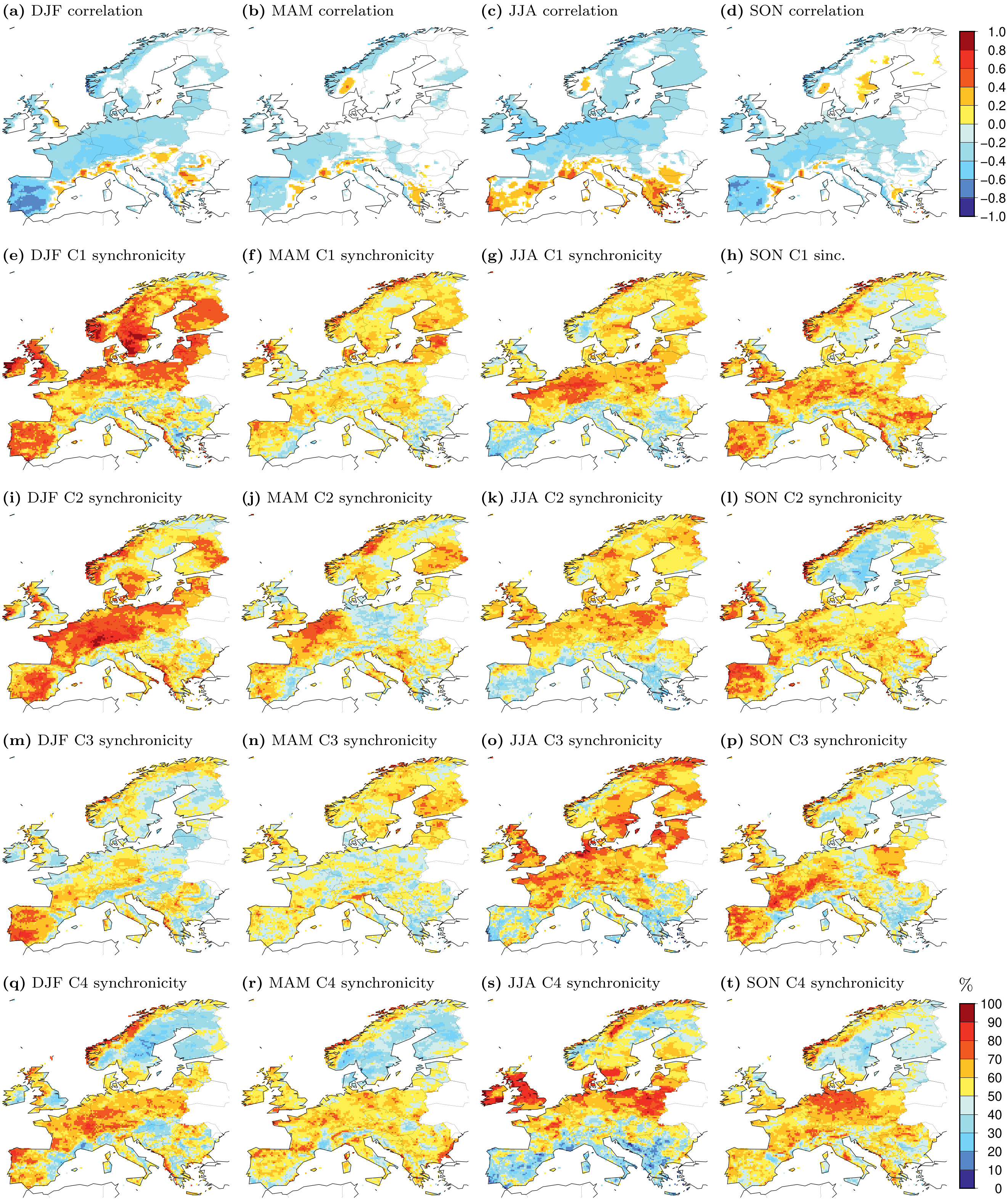
(a) DJF correlation
(b) MAM correlation
(c) JJA correlation
(d) SON correlation
1.0
0.8
0.6
0.4
0.2
0.0
−0.2
−0.4
−0.6
−0.8
−1.0
(e) DJF C1 synchronicity
(f) MAM C1 synchronicity
(g) JJA C1 synchronicity
(h) SON C1 sinc.
(i) DJF C2 synchronicity
(j) MAM C2 synchronicity
(k) JJA C2 synchronicity
(l) SON C2 synchronicity
(m) DJF C3 synchronicity
(n) MAM C3 synchronicity
(o) JJA C3 synchronicity
(p) SON C3 synchronicity
(q) DJF C4 synchronicity
(r) MAM C4 synchronicity
(s) JJA C4 synchronicity
(t) SON C4 synchronicity
%
100
90
80
70
60
50
40
30
20
10
0

Figure 4.

should be assured at the same time. As indicated in Section 2.4, this condition was imposed here to guarantee that the mean annual cycle of production under the optimized solutions is equal to or better than that obtained from the ERA5-based capacity factor series under a baseline (BASE) scenario in which the current regional shares of both energies, as informed in IRENA (2020) and provided here in Table 1, are evenly distributed across the regions.

In a first step, sub-regions with homogeneous temporal variability in the time series of monthly capacity factor anomalies are identified for each energy and each target region separately (Figure 5, first and third columns). These sub-regions are to a large extent dictated by the atmospheric conditions (i.e., the mixed influences of the atmospheric patterns considered above), therefore accounting for the climate-driven spatial heterogeneity in the assessed fields. Sub-regional mean series of solar and wind capacity factors are then generated by simply taking the average of the local series over all grid points embedded in the sub-region. In that way, this first step also reduces the dimensionality (number of degrees of freedom) of the optimization problem to be solved in the next step. Moreover, this approach ensures the viability of the optimal scenarios of installations that will be generated with the optimization process: as long as the identified sub-regions are large enough, there is no need to take into account the feasibility of individual projects at particular locations.

In a second step, standard optimization techniques are applied to exploit the full potential of the spatio-temporal complementarity of the resources and throw the optimal shares of each technology in each sub-region. The aim is to identify the sub-regional shares that minimize the variance of the monthly anomalies of the resulting wind-plus-solar power production (per unit of installed power capacity) at regional level, without losses in the mean regional capacity factor. This is done under the two frameworks described above, OD and ODS. In the OD approach, the regional shares of wind and solar power remain at their current values, as in the BASE scenario (note that BASE is included in the solution space sampled by OD). In the ODS experiment, the regional shares of wind and solar power come also into the optimization game with the only restriction that the most profitable of these two energies, in regional average terms, should have a larger penetration than the other in the region. That way here we adopted the sound assumption that if a region is richer in sun than in wind, energy policies will allocate more resources for deploying solar installations than for investing in wind generation (as it actually occurs in all regions but R1; see Table 1). Therefore, this experiment further informs on the sub-regional and regional shares of each energy that should be pursued to guarantee the most stable production. By working on optimal distributions and shares simultaneously, the ODS can yield a different spatial distribution of the resources as compared to OD, even for those regions where the OD scenario is in the solution space of ODS (R2-to-R5, see Table 1).

The results of these two optimization exercises are provided in Figure 5 for each region (rows). Bars in the second/fourth column display the optimal shares of solar/wind power in each sub-region, using the same color code as the one in the accompanying map (first/third column). For each exercise, the sum of the total regional share of solar power plus the total regional share of wind power must be 100%. For instance, in R1 (Iberia), the current regional share of solar power is 24% and that of wind power is 76%, and so the OD bars in Figures 5b and 5d reach exactly these values. In the ODS exercise, these values can be modified during the optimization process. Following with R1, the optimal total regional share of solar power grows above 70% and so the optimal total regional share of wind power falls below 30% (Figures 5b and 5d), meaning a radical transformation of the current energy mix, with substantial investments toward solar facilities. This increase of the optimal solar power share at the expense of the optimal wind power share as compared to current values occurs similarly, although less pronounced, in all the studied regions. The results of the ODS exercise must be interpreted taking into account that the solution space is restricted by the imposed constraint on the level of penetration, which benefits the most profitable resource. Accordingly, the solar power share must be greater than the wind power share in those regions where the solar resource is more abundant (R1 and R2), whereas the opposite applies for the remaining regions (R3, R4 and R5; see Table 1). Hence, the growth of the solar power share was actually forced to exceed

Figure 4. *Synchronicity of the solar and wind power anomalies*. First row shows the temporal correlation (when statistically significant, $p < 0.05$) between the time series of monthly anomalies in the solar and wind power capacity factor for each season (December-to-February [DJF], March-to-May [MAM], June-to-August [JJA] or September-to-November [SON] months of 1979–2020). The statistical significance of the correlations was assessed using the R *cor.test* function (https://www.rdocumentation.org/packages/stats/versions/3.6.2/topics/cor.test; two-sided). Second to fifth rows show the synchronicity index, defined as the percentage of time within each season when the anomalies of solar and wind power capacity factors have different sign under the influence of different recurrent atmospheric patterns (C1–C4 from top to bottom). The studied area is restricted here to that of Figure 2.

10.1029/2022EF003332

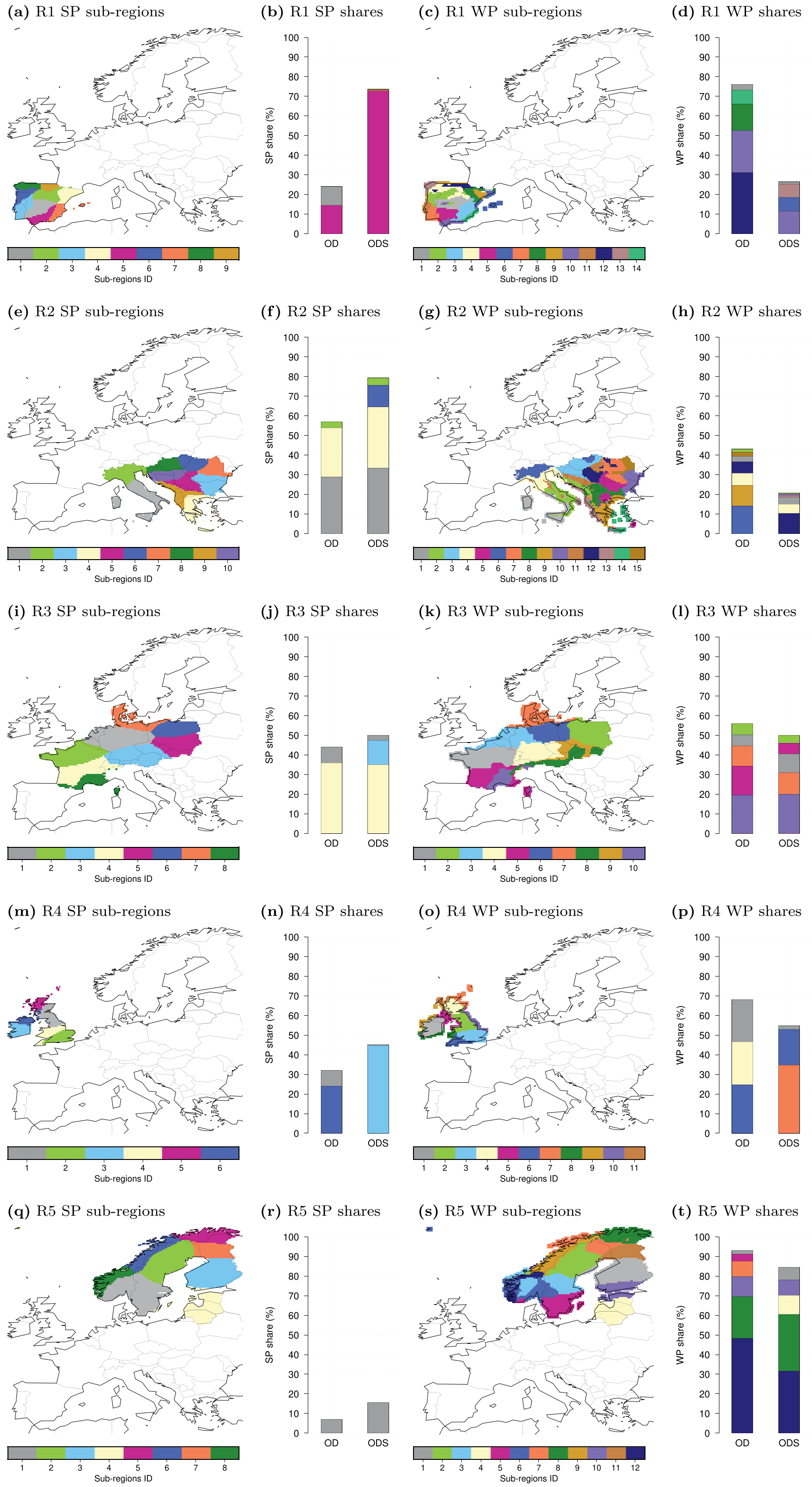

Figure 5. *Optimal sub-regional shares*. For each region (R1–R5; rows), colored maps show the sub-regions (clusters of grid points) with homogeneous temporal variability in the monthly anomalies series of the solar (SP, first column) and wind power (WP, third column) capacity factor. Boxes to the right of each map panel indicate the sub-regional shares (in %) of SP (second column) and WP (fourth column) that minimize the variance of the total wind-plus-solar regional production under the Optimal Distributions (OD) and Optimal Distributions and Shares (ODS) criteria. The sum of the total SP share and the total WP share should be 100% for each scenario (OD and ODS).

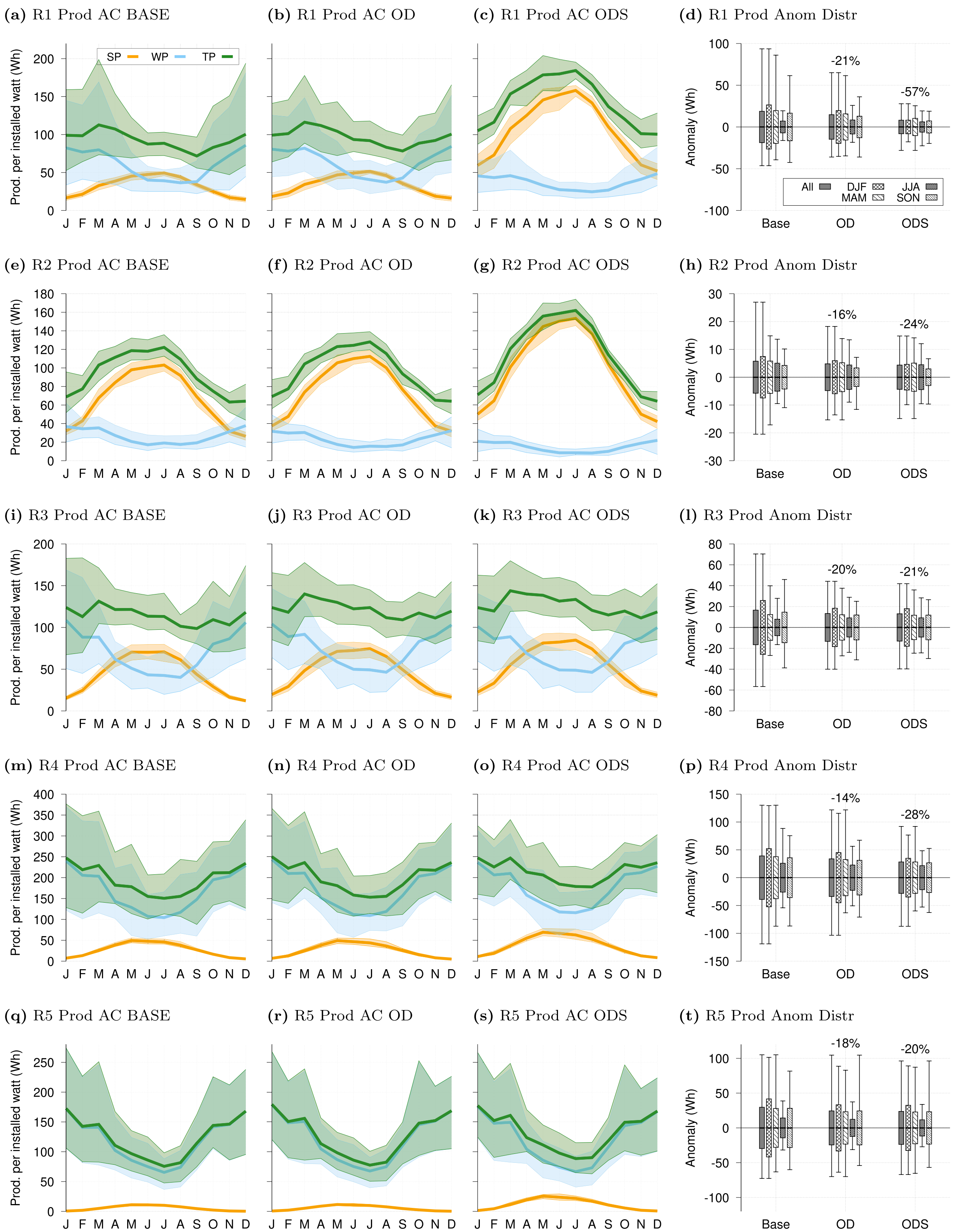
(a) R1 Prod AC BASE
(b) R1 Prod AC OD
(c) R1 Prod AC ODS
(d) R1 Prod Anom Distr
(e) R2 Prod AC BASE
(f) R2 Prod AC OD
(g) R2 Prod AC ODS
(h) R2 Prod Anom Distr
(i) R3 Prod AC BASE
(j) R3 Prod AC OD
(k) R3 Prod AC ODS
(l) R3 Prod Anom Distr
(m) R4 Prod AC BASE
(n) R4 Prod AC OD
(o) R4 Prod AC ODS
(p) R4 Prod Anom Distr
(q) R5 Prod AC BASE
(r) R5 Prod AC OD
(s) R5 Prod AC ODS
(t) R5 Prod Anom Distr
SP
WP
TP
All
DJF
MAM
JJA
SON
Prod. per installed watt (Wh)
Anomaly (Wh)
J F M A M J J A S O N D
Base
OD
ODS
-21%
-57%
-16%
-24%
-20%
-21%
-14%
-28%
-18%
-20%

Figure 6.

50% in R1 (from its current 24%), but limited to remain below 50% in R3, R4 and R5 (note that the ODS scenario for R3 reaches this limit).

Finally, we evaluate the benefits of the optimized scenarios depicted in Figure 5 by comparison with the BASE scenario mentioned above. For the three scenarios (BASE, OD and ODS), Figure 6 (first, second and third columns, respectively) provides the mean annual cycles (with thick lines) of the solar (in yellow), wind (in blue), and total wind-plus-solar (in green) capacity factor (i.e., production per installed watt). Shading represents the maximum range of variation of all the monthly records in the series (in the period 1979–2020). Note that the optimization looks for a reduction of the width of the green shadow, importantly without losses in the mean capacity factor. The latter means that the green thick line in the optimized scenarios should always be above that of the BASE scenario, while reducing, at the same time, the green shaded interval, as it does occur. Given the current regional shares, all regions have room for improvement through a redistribution of their sub-regional shares (compare BASE with OD). Some regions, in particular R3 and R5, are actually on their path toward the optimal balance of wind and solar resources (i.e., with similar OD and ODS scenarios). Others, mainly those of southern Europe and the UK, still have a long way ahead, but also the unique opportunity to experience the largest growth in stability of their power potential. Sunny southern areas are among the regions with the largest solar capacity factors in summer (the season with overall lower production), which, in fact, grow substantially in the optimized solutions (compare the thick green line in panels a and c and panels e and g in Figure 6). Besides, from a pan-European strategy perspective, they seem key to guarantee a stabilized power.

To quantify the benefits of the optimized scenarios in terms of stabilized production, the last column of Figure 6 (gray shaded bar) depicts the distribution of the monthly anomalies in wind-plus-solar production series for each scenario (BASE, OD and ODS). With the OD approach, the range of these anomalies, as measured by their variance, is reduced by 15%–20% in all the studied regions. This is achieved just by an optimal distribution of the current regional shares of each technology. This reduction grows up to 60% in R1, 20%–25% in the other regions, with the ODS approach, that is, if these regional shares come also into the optimization process. Note that the optimization has been applied considering all monthly records in the series. Hence, the reported improvements would not necessarily have to happen equally for the four seasons. However, if seasonal subsets of the regional series are assessed separately (hatched bars in the last column of Figure 6), all regions do attain reduced variances through almost all of the year.

4. Conclusions and Discussion

Renewable energies, in particular wind and solar power, are at the forefront of the fight against climate change and energy threats. Their integration in the energy mix enlarges its vulnerability to climate variability and change, and thus requires smart strategies to hamper undesired fluctuations and blackout episodes. Here we present a novel climate-informed methodology aimed to help planning the deployment of new renewables units with the goal of reducing the intermittency of the joint production from solar photovoltaic and wind power. It takes advantage of their spatio-temporal complementarity, which, at monthly scales, is largely determined by well-known recurrent atmospheric patterns, as we showed here. The method, implemented in an open-access user-friendly and customizable tool called CLIMAX (http://climax.inf.um.es/), has been proven here in an illustrative pilot study over pan-European regions for which the temporal variability of the monthly wind-plus-solar production is to be reduced. However, it has been designed so that actual needs and circumstances can be taken into account for practical applications and guidance. The target spatial domain and temporal scale (at which the temporal variability of the production is to be reduced) are eligible fields, the total shares of each technology

Figure 6. *Evaluation of the optimized scenarios*. Per regions (R1–R5; rows), colored plots show the 1979–2020 mean annual cycles of production (thick lines) from solar power (SP, orange), wind power (WP, blue) and total (wind-plus-solar) power (TP, green) per installed watt (units: Wh) under three different scenarios: BASE, Optimal Distributions (OD) and Optimal Distributions and Shares (ODS) (first to third column, respectively). Shadows in these plots represent the maximum range of variation of the individual records in the series. Black and white plots (fourth column) show boxplots with the distributions of the TP monthly anomalies (units: Wh) for 1979–2020 under each scenario (BASE, OD and ODS) considering all the records in the series (shaded boxplots) or only the records corresponding to each season (hatched boxplots, December-to-February [DJF], March-to-May [MAM], June-to-August [JJA] or September-to-November [SON] months). Box limits represent one standard deviation of the series above and below its mean value (shown with thick horizontal lines, null here). Whisker limits represent the maximum deviation of the individual records in the TP monthly anomaly series. Numbers above the OD and ODS boxplots indicate the associated reduction in the standard deviation of the TP monthly anomaly series (considering all the records in the series and expressed in relative terms, in % with respect to the BASE scenario).

can be fixed, forced to stay above/below certain thresholds or let free to find their optimum, and the minimum production to be guaranteed can be modified. It can also be employed to minimize the variability of the residual load, not necessarily that of the total production, as we did here. According to the specifications, the tool provides optimum shares of each technology over a number of sub-regions in which the target domain has previously been divided automatically, which should constitute a guide for long-term planning. Also, an additional code is made available on the webpage to find optimum locations for new installations given that the current spatial distribution of installations is known (see Section 2.4), which might be the most useful application of the tool for the short-term decision making.

Despite the experimental and pilot nature of the CLIMAX application presented here, our results indicate that all European regions considered should make efforts in their energy policies toward the deployment of more solar facilities in order to reduce the month-to-month volatility of the combined wind-solar production. The benefits would be huge, particularly for southern European regions and at pan-European level. Still, there are a number of caveats to keep in mind. First of all, regarding the particular solutions presented here, having a large percentage of production based on solar power means low production rates at nighttime, which would require the use of energy storage systems with large capacities. In fact, the optimal shares and units distribution at a certain time-scale is likely to be non-optimal for others time-scales (Wohland et al., 2021), and so recursive applications of the method might need to be performed over prioritized time-scales, for instance. It would be likewise worth addressing solutions accommodating the variability of the renewable production to the peak net load hours or to the seasons when hydropower is unavailable. Besides, although previous works determined a small impact of climate change on the statistics of the wind and solar powers for the coming decades, specifically over some European regions (Jerez et al., 2015, 2019; Tobin et al., 2015, 2016), it cannot be assured that the CLIMAX-optimal scenario under current climate conditions will still hold under a changed climate. On the other side, altered climates can infer shifts in the demand curves and so in the grid supply requirements (Bloomfield et al., 2021; Garrido-Pérez et al., 2021; Van Ruijven et al., 2019), which may also compromise strategies made upon the business-as-usual assumption. Moreover, short and medium range climate variability, such as that characterized through weather regimes, affects both the renewable capacity factors and the electricity demand simultaneously (e.g., Bloomfield et al., 2020; van der Wiel et al., 2019). In this sense, it may not be sufficient to ensure a mean production (e.g., that a certain percentage of the mean annual cycle of the demand will be satisfied, as we impose here) but a minimum production at every time step in the series (the codes do allow for so) or under the various foreseeable weather situations. More generally, mean climate conditions could suffer changes over the period used to design the scenarios (here the last 42 years), which could affect the stability of the solutions. The issue of the stability of the wind-solar complementarity over long periods remains largely unexplored so far, and also out of the scope of this contribution. In another vein, it is clear that the wider the target domain, the better the spatio-temporal complementarity among the resources works (e.g., Jerez et al., 2019). However, it comes at the expense of transmission and energy-market issues that need to be carefully considered in practical applications.

With its limitations, this contribution poses a substantial step forward over previous works that provided strictly academic research about the spatio-temporal complementarity of both powers (e.g., Garrido-Pérez et al., 2020; Jerez et al., 2013b; Jerez & Trigo, 2013; van der Wiel et al., 2019), focused on a single attribute of their compound complementarity (e.g., Costoya et al., 2022; Couto & Estanqueiro, 2021; Jánosi et al., 2021; Liu et al., 2020; Mühlemann et al., 2022), or used national aggregate capacity factors in their analysis, thus masking the richness of spatial climatic variability over such predefined regions (Frank et al., 2021; Grams et al., 2017; Santos-Alamillos et al., 2017; Wohland et al., 2021). Making use of this previous knowledge, CLIMAX has been designed to take a transferable advantage of the full spatio-temporal complementarity between wind and solar powers, with practical applications beyond the limits of the illustrative exercise presented here.

Data Availability Statement

The ERA5 (Hersbach et al., 2020) data used in this study can be downloaded from the Climate Data Store webpage (https://cds.climate.copernicus.eu).
Codes used in this study can be downloaded from http://climax.inf.um.es/ and Zenodo (Jerez & Somoza, 2023).

Acknowledgments

This study was supported by the Grant TED2021-131074B-I00 funded by MCIN/AEI/10.13039/501100011033 and cofunded by the European Union NExt-GenerationEU/PRTR, the EASE project (RTI2018-100870-A-I00, MCIU/AEI/FEDER, UE) and the CLIMAX project (20642/JLI/18, Fundación Séneca–Agencia de Ciencia y Tecnología de la Región de Murcia). S. J. acknowledges funding by the Spanish Ministry of Science, Innovation and Universities Ramón y Cajal Grant Reference RYC2020-029993-I. M. T. acknowledges funding by the Spanish Ministry of Science, Innovation and Universities Ramón y Cajal Grant Reference RYC2019-027115-I. A. M. S. acknowledges support by AEI (Spain)/FEDER (EU) Grant PID2019-104272RB-C52/AEI/10.13039/501100011033. D. B. was supported by the H2020 EU project CLINT (Grant Agreement 101003876) and the European Union NExtGenerationEU (Regulation EU 2020/2094), through CSIC's Interdisciplinary Thematic Platform Clima (PTI Clima)/Development of Operational Climate Services.

References

Antonini, E. G., Ruggles, T. H., Farnham, D. J., & Caldeira, K. (2022). The quantity-quality transition in the value of expanding wind and solar power generation. *iScience*, *25*(4), 104140. https://doi.org/10.1016/j.isci.2022.104140

Bloomfield, H. C., Brayshaw, D. J., & Charlton-Perez, A. J. (2020). Characterizing the winter meteorological drivers of the European electricity system using targeted circulation types. *Meteorological Applications*, *27*(1), e1858. https://doi.org/10.1002/met.1858

Bloomfield, H. C., Brayshaw, D. J., Troccoli, A., Goodess, C. M., De Felice, M., Dubus, L., et al. (2021). Quantifying the sensitivity of European power systems to energy scenarios and climate change projections. *Renewable Energy*, *164*, 1062–1075. https://doi.org/10.1016/j.renene.2020.09.125

Brown, P. T., Farnham, D. J., & Caldeira, K. (2021). Meteorology and climatology of historical weekly wind and solar power resource droughts over western North America in ERA5. *SN Applied Sciences*, *3*(10), 1–12. https://doi.org/10.1007/s42452-021-04794-z

Cassou, C., Terray, L., & Phillips, A. S. (2005). Tropical Atlantic influence on European heat waves. *Journal of Climate*, *18*(15), 2805–2811. https://doi.org/10.1175/jcli3506.1

Cattell, R. B. (1966). The Scree test for the number of factors. *Multivariate Behavioral Research*, *1*(2), 245–276. https://doi.org/10.1207/s15327906mbr0102_10

Cortesi, N., Torralba, V., Lledó, L., Manrique-Suñén, A., Gonzalez-Reviriego, N., Soret, A., & Doblas-Reyes, F. J. (2021). Yearly evolution of Euro-Atlantic weather regimes and of their sub-seasonal predictability. *Climate Dynamics*, *56*(11), 3933–3964. https://doi.org/10.1007/s00382-021-05679-y

Costoya, X., DeCastro, M., Carvalho, D., Arguilé-Pérez, B., & Gómez-Gesteira, M. (2022). Combining offshore wind and solar photovoltaic energy to stabilize energy supply under climate change scenarios: A case study on the western Iberian Peninsula. *Renewable and Sustainable Energy Reviews*, *157*, 112037. https://doi.org/10.1016/j.rser.2021.112037

Couto, A., & Estanqueiro, A. (2021). Assessment of wind and solar PV local complementarity for the hybridization of the wind power plants installed in Portugal. *Journal of Cleaner Production*, *319*, 128728. https://doi.org/10.1016/j.jclepro.2021.128728

European Commission. (2019). The European Green Deal.

Folland, C. K., Knight, J., Linderholm, H. W., Fereday, D., Ineson, S., & Hurrell, J. W. (2009). The summer North Atlantic Oscillation: Past, present, and future. *Journal of Climate*, *22*(5), 1082–1103. https://doi.org/10.1175/2008jcli2459.1

Frank, C., Fiedler, S., & Crewell, S. (2021). Balancing potential of natural variability and extremes in photovoltaic and wind energy production for European countries. *Renewable Energy*, *163*, 674–684. https://doi.org/10.1016/j.renene.2020.07.103

Garrido-Pérez, J. M., Barriopedro, D., García-Herrera, R., & Ordóñez, C. (2021). Impact of climate change on Spanish electricity demand. *Climatic Change*, *165*(3), 1–18. https://doi.org/10.1007/s10584-021-03086-0

Garrido-Pérez, J. M., Ordóñez, C., Barriopedro, D., García-Herrera, R., & Paredes, D. (2020). Impact of weather regimes on wind power variability in Western Europe. *Applied Energy*, *264*, 114731. https://doi.org/10.1016/j.apenergy.2020.114731

Grams, C. M., Beerli, R., Pfenninger, S., Staffell, I., & Wernli, H. (2017). Balancing Europe's wind-power output through spatial deployment informed by weather regimes. *Nature Climate Change*, *7*(8), 557–562. https://doi.org/10.1038/nclimate3338

Hartigan, J. A., & Wong, M. A. (1979). Algorithm AS 136: A k-means clustering algorithm. *Journal of the Royal Statistical Society. Series C (Applied Statistics)*, *28*(1), 100–108. https://doi.org/10.2307/2346830

Hersbach, H., Bell, B., Berrisford, P., Hirahara, S., Horányi, A., Muñoz-Sabater, J., et al. (2020). The ERA5 global reanalysis. *Quarterly Journal of the Royal Meteorological Society*, *146*(730), 1999–2049. https://doi.org/10.1002/qj.3803

IPCC. (2018). In V. Masson-Delmotte, P. Zhai, H.-O. Pörtner, D. Roberts, J. Skea, et al. (Eds.). *Global warming of 1.5°C*. An IPCC Special Report on the impacts of global warming of 1.5°C above pre-industrial levels and related global greenhouse gas emission pathways, in the context of strengthening the global response to the threat of climate change, sustainable development, and efforts to eradicate poverty. Cambridge University Press.

IPCC. (2021). In V. Masson-Delmotte, P. Zhai, A. Pirani, S. L. Connors, C. Péan, et al. (Eds.), *Climate change 2021: The physical science basis. Contribution of Working Group I to the sixth assessment report of the Intergovernmental Panel on Climate Change*. Cambridge University Press.

IPCC. (2022). In P. R. Shukla, J. Skea, R. Slade, A. Al Khourdajie, R. van Diemen, et al. (Eds.), *Climate change 2022: Mitigation of climate change. Contribution of Working Group III to the sixth assessment report of the Intergovernmental Panel on Climate Change*. Cambridge University Press.

IRENA. (2020). *Renewable capacity statistics 2020*. International Renewable Energy Agency (IRENA).

Jánosi, I. M., Medjdoub, K., & Vincze, M. (2021). Combined wind-solar electricity production potential over North-Western Africa. *Renewable and Sustainable Energy Reviews*, *151*, 111558. https://doi.org/10.1016/j.rser.2021.111558

Jerez, S., & Somoza, A. (2023). soniajerez/CLIMAX: CLIMAX. April 22, 2023 Release (Version 1.0) [Software]. Zenodo. https://doi.org/10.5281/zenodo.7854945

Jerez, S., Tobin, I., Turco, M., Jiménez-Guerrero, P., Vautard, R., & Montávez, J. P. (2019). Future changes, or lack thereof, in the temporal variability of the combined wind-plus-solar power production in Europe. *Renewable Energy*, *139*, 251–260. https://doi.org/10.1016/j.renene.2019.02.060

Jerez, S., Tobin, I., Vautard, R., Montávez, J. P., López-Romero, J. M., Thais, F., et al. (2015). The impact of climate change on photovoltaic power generation in Europe. *Nature Communications*, *6*(1), 1–8. https://doi.org/10.1038/ncomms10014

Jerez, S., & Trigo, R. M. (2013). Time-scale and extent at which large-scale circulation modes determine the wind and solar potential in the Iberian Peninsula. *Environmental Research Letters*, *8*(4), 044035. https://doi.org/10.1088/1748-9326/8/4/044035

Jerez, S., Trigo, R. M., Sarsa, A., Lorente-Plazas, R., Pozo-Vázquez, D., & Montávez, J. P. (2013a). Spatio-temporal complementarity between solar and wind power in the Iberian Peninsula. *Energy Procedia*, *40*, 48–57. https://doi.org/10.1016/j.egypro.2013.08.007

Jerez, S., Trigo, R. M., Vicente-Serrano, S. M., Pozo-Vázquez, D., Lorente-Plazas, R., Lorenzo-Lacruz, J., et al. (2013b). The impact of the North Atlantic Oscillation on renewable energy resources in southwestern Europe. *Journal of Applied Meteorology and Climatology*, *52*(10), 2204–2225. https://doi.org/10.1175/jamc-d-12-0257.1

Jourdier, B. (2020). Evaluation of ERA5, MERRA-2, COSMO-REA6, NEWA and AROME to simulate wind power production over France. *Advances in Science and Research*, *17*, 63–77. https://doi.org/10.5194/asr-17-63-2020

Liu, L., Wang, Z., Wang, Y., Wang, J., Chang, R., He, G., et al. (2020). Optimizing wind/solar combinations at finer scales to mitigate renewable energy variability in China. *Renewable and Sustainable Energy Reviews*, *132*, 110151. https://doi.org/10.1016/j.rser.2020.110151

Lledó, L., Torralba, V., Soret, A., Ramon, J., & Doblas-Reyes, F. J. (2019). Seasonal forecasts of wind power generation. *Renewable Energy*, *143*, 91–100. https://doi.org/10.1016/j.renene.2019.04.135

Lorente-Plazas, R., Montávez, J. P., Jerez, S., Gómez-Navarro, J. J., Jiménez-Guerrero, P., & Jiménez, P. A. (2015). A 49 year hindcast of surface winds over the Iberian Peninsula. *International Journal of Climatology*, *35*(10), 3007–3023. https://doi.org/10.1002/joc.4189

Michelangeli, P. A., Vautard, R., & Legras, B. (1995). Weather regimes: Recurrence and quasi stationarity. *Journal of the Atmospheric Sciences*, *52*(8), 1237–1256. https://doi.org/10.1175/1520-0469(1995)052<1237:wrraqs>2.0.co;2

Mühlemann, D., Folini, D., Pfenninger, S., Wild, M., & Wohland, J. (2022). Meteorologically-informed spatial planning of European PV deployment to reduce multiday generation variability. *Earth's Future*, *10*(7), e2022EF002673. https://doi.org/10.1029/2022ef002673

Olauson, J. (2018). ERA5: The new champion of wind power modelling? *Renewable Energy*, *126*, 322–331. https://doi.org/10.1016/j.renene.2018.03.056

Santos-Alamillos, F. J., Brayshaw, D. J., Methven, J., Thomaidis, N. S., Ruiz-Arias, J. A., & Pozo-Vázquez, D. (2017). Exploring the meteorological potential for planning a high performance European electricity super-grid: Optimal power capacity distribution among countries. *Environmental Research Letters*, *12*(11), 114030. https://doi.org/10.1088/1748-9326/aa8f18

Schindler, D., Behr, H. D., & Jung, C. (2020). On the spatiotemporal variability and potential of complementarity of wind and solar resources. *Energy Conversion and Management*, *218*, 113016. https://doi.org/10.1016/j.enconman.2020.113016

Solomon, A. A., Child, M., Caldera, U., & Breyer, C. (2020). Exploiting wind-solar resource complementarity to reduce energy storage need. *AIMS Energy*, *8*(5), 749–770. https://doi.org/10.3934/energy.2020.5.749

Tobin, I., Jerez, S., Vautard, R., Thais, F., Van Meijgaard, E., Prein, A., et al. (2016). Climate change impacts on the power generation potential of a European mid-century wind farms scenario. *Environmental Research Letters*, *11*(3), 034013. https://doi.org/10.1088/1748-9326/11/3/034013

Tobin, I., Vautard, R., Balog, I., Bréon, F. M., Jerez, S., Ruti, P. M., et al. (2015). Assessing climate change impacts on European wind energy from ENSEMBLES high-resolution climate projections. *Climatic Change*, *128*(1), 99–112. https://doi.org/10.1007/s10584-014-1291-0

Urraca, R., Huld, T., Gracia-Amillo, A., Martinez-de-Pison, F. J., Kaspar, F., & Sanz-Garcia, A. (2018). Evaluation of global horizontal irradiance estimates from ERA5 and COSMO-REA6 reanalyses using ground and satellite-based data. *Solar Energy*, *164*, 339–354. https://doi.org/10.1016/j.solener.2018.02.059

van der Wiel, K., Bloomfield, H. C., Lee, R. W., Stoop, L. P., Blackport, R., Screen, J. A., & Selten, F. M. (2019). The influence of weather regimes on European renewable energy production and demand. *Environmental Research Letters*, *14*(9), 094010. https://doi.org/10.1088/1748-9326/ab38d3

Van Ruijven, B. J., De Cian, E., & Sue Wing, I. (2019). Amplification of future energy demand growth due to climate change. *Nature Communications*, *10*(1), 1–12. https://doi.org/10.1038/s41467-019-10399-3

von Storch, H., & Zwiers, F. W. (2002). *Statistical analysis in climate research*. Cambridge University press.

Ward, J. H., Jr. (1963). Hierarchical grouping to optimize an objective function. *Journal of the American Statistical Association*, *58*(301), 236–244. https://doi.org/10.1080/01621459.1963.10500845

Wilks, D. S. (2006). *Statistical methods in the atmospheric sciences*. Academic Press.

Wohland, J., Brayshaw, D., & Pfenninger, S. (2021). Mitigating a century of European renewable variability with transmission and informed siting. *Environmental Research Letters*, *16*(6), 064026. https://doi.org/10.1088/1748-9326/abff89